JOURNAL OF THE AMERICAN COLLEGE OF CARDIOLOGY
© 2017 BY THE AMERICAN COLLEGE OF CARDIOLOGY FOUNDATION
PUBLISHED BY ELSEVIER

VOL. 70, NO. 22, 2017
ISSN 0735-1097/$36.00
https://doi.org/10.1016/j.jacc.2017.09.1107

Optogenetic Modulation of Cardiac Sympathetic Nerve Activity to Prevent Ventricular Arrhythmias

Lilei Yu, MD, PhD,[a,b,c] Liping Zhou, MD,[a,b,c] Gang Cao, MD, PhD,[d,e] Sunny S. Po, MD, PhD,[f] Bing Huang, MD, PhD,[a,b,c] Xiaoya Zhou, MD, PhD,[a,b,c] Menglong Wang, MD,[a,b,c] Shenxu Yuan, MD,[a,b,c] Zhuo Wang, MD,[a,b,c] Songyun Wang, MD,[a,b,c] Hong Jiang, MD, PhD[a,b,c]

ABSTRACT

BACKGROUND Studies have shown that left stellate ganglion (LSG) suppression protects against ventricular arrhythmias (VAs). Optogenetics is a novel technique to reversibly regulate the activity of the targeted neurons.

OBJECTIVES This study aimed to investigate whether an optogenetically silenced LSG could protect against VAs induced by myocardial ischemia.

METHODS Adeno-associated virus (AAV) was used as the vector to deliver ArchT, an inhibitory light-sensitive opsin, to the LSG neurons. Twenty male beagles were randomized into the optogenetics group (n = 10, AAV2/9-CAG-ArchT-GFP microinjected into LSG) and control group (n = 10, AAV2/9-CAG-GFP microinjected into LSG). After 4 weeks, the LSG function and neural activity, heart rate variability, ventricular action potential duration, and effective refractory period were measured in the absence or presence of a light-emitting diode illumination (565 nm). Myocardial ischemia was induced by left anterior coronary artery ligation and 1 h of electrocardiography was recorded for VAs analysis.

RESULTS ArchT was successfully expressed in all dogs. Transient light-emitting diode illumination significantly suppressed the LSG function, LSG neural activity, and sympathetic nerve indices of heart rate variability as well as prolonged left ventricular effective refractory period and APD90 only in the optogenetics group. Thirty-minute illumination further enhanced these changes in the optogenetics group. Importantly, all of these changes returned to baseline within 2 h after illumination was turned off. Moreover, the ischemia-induced VAs were significantly suppressed by illumination only in the optogenetics group.

CONCLUSIONS Optogenetic modulation could reversibly inhibit the neural activity of LSG, thereby increasing electrophysiological stability and protecting against myocardial ischemia–induced VAs. (J Am Coll Cardiol 2017;70:2778–90) © 2017 by the American College of Cardiology Foundation.

Malignant ventricular arrhythmias (VAs) remain a major contributor to sudden cardiac death in patients with myocardial ischemia (1,2). It is well established that the cardiac sympathetic nervous system, particularly the left stellate ganglion (LSG), plays a prominent role in modulating ventricular electrophysiology and arrhythmias (3–5). Left cardiac sympathetic denervation has been applied to treat animals or patients with life-threatening VAs such as post-myocardial

Listen to this manuscript's audio summary by *JACC* Editor-in-Chief Dr. Valentin Fuster.

From the [a]Department of Cardiology, Renmin Hospital of Wuhan University, Wuhan, China; [b]Cardiovascular Research Institute, Wuhan University, Wuhan, China; [c]Hubei Key Laboratory of Cardiology, Wuhan, China; [d]Biomedical Center of Huazhong Agricultural University, Wuhan, China; [e]College of Veterinary Medicine, Huazhong Agricultural University, Wuhan, China; and the [f]Heart Rhythm Institute and Department of Medicine, University of Oklahoma Health Sciences Center, Oklahoma City, Oklahoma.
This work was supported by the grants from the National Nature Science Foundation of China (Nos. 81530011, 81570463, and 81600395), the Natural Science Foundation of Hubei Province (Nos. 2016CFA065, 2016CFA048, and 2016CFB621), and the Fundamental Research Funds of Wuhan City (No. 2016070204010134). The authors have reported that they have no relationships relevant to the contents of this paper to disclose. Drs. Yu, Zhou, and Cao contributed equally to this work and are joint first authors.

Manuscript received February 25, 2017; revised manuscript received September 5, 2017, accepted September 26, 2017.

infarction refractory VAs or electrical storm, long QT syndrome, and catecholaminergic polymorphic ventricular tachycardia (VT) (6–9). Optogenetics is a novel technology that is widely used in the neuroscience field for silencing or enhancing the activity of genetically targeted neurons (10,11). When ArchT, an inhibitory light-sensitive opsin, is genetically expressed in targeted cells and activated by illumination with the appropriate wavelength, it induces hyperpolarizing currents, thus silencing the cells (12–14). In the present study, we aimed to develop a novel optogenetic approach in which an adeno-associated virus (AAV) carrying the ArchT gene was transfected to the LSG neurons. The LSG function and neural activity as well as ventricular electrophysiological properties and VAs in response to myocardial ischemia challenges were evaluated.

SEE PAGE 2791

METHODS

ANIMAL PREPARATION. Twenty adult male beagles (body weight 10 to 12 kg) included in this study were supplied by the Center of Experimental Animals in the Medical College of Wuhan University. This study was performed in accordance with the recommendations in the Guide for the Care and Use of Laboratory Animals of the National Institutes of Health. The protocol was approved by the Committee on the Ethics of Animal Experiments of Wuhan University. All dogs were anesthetized with Na-pentobarbital (30 mg/kg) and ventilated with room air by a positive pressure respirator (MAO01746, Harvard Apparatus, Holliston, Massachusetts). Additional maintenance doses of 60 mg/h Na-pentobarbital were administered during the procedure. Normal saline at 100 ml/h was infused to replace spontaneous fluid losses. Left femoral artery catheterization was performed to monitor systemic arterial pressure. Body surface electrocardiography (ECG) was recorded with a computer-based Laboratory System (Lead 7000, Jinjiang, Chengdu, China). A heating pad was used to maintain a core body temperature of 36.5 ± 0.5°C. All efforts were made to minimize discomfort.

VIRAL INJECTION INTO LSG. Twenty dogs were randomly divided into the optogenetics group and the control group (Figure 1A). The virus AAV2/9-CAG-ArchT-GFP was chosen for transfecting the LSG. A similar construct (AAV2/9-CAG-GFP) without ArchT was used as a control. The virus was purchased from OBio (Shanghai, China). After anesthesia, a left thoracotomy was performed at the third intercostal space. The LSG was carefully exposed and virus solution (AAV2/9-CAG-ArchT-GFP: 20 μl, 6.25 × 1,012 vector genomes/ml; AAV2/9-CAG-GFP: 20 μl, 5.66 × 1,012 vector genomes/ml) were injected into 4 sites using a 30-G beveled needle (Figure 1B). Virus solution was injected at 1 μl/min, using a 25-μl Hamilton syringe connected to a Harvard PHD syringe pump (Harvard Apparatus). After the injection, the chest was closed in layers and antibiotics (penicillin sodium) were administered for 3 days after surgery.

IMPLANTATION OF THE LIGHT-EMITTING DIODE DEVICE. Four weeks after viral injection, a left thoracotomy was conducted at the fourth intercostal space to expose the heart and LSG. A 2-cm coupled monochromatic light-emitting diode (LED) (565 nm, Convergence Technology, Wuhan, China) was inserted and implanted into the chest wall near the LSG (Figure 1C). The LED was connected externally to the monochromatic LED system (Convergence Technology) for illumination. According to previous studies (15,16), the LSG was illuminated with fixed illumination parameter (40% duty cycle, 20-Hz period, 20-ms pulse width, 3 to 5 mW/mm^2) to reduce heat generation while ensuring the illumination efficiency. All electrophysiological parameters in vivo were measured in the absence or presence of LSG illumination.

MEASUREMENT OF THE LSG FUNCTION. LSG function was assessed by the maximal systolic blood pressure (BP) change induced by high-frequency (HF) stimulation (20 Hz, 0.1-ms pulse duration) using a Grass-S88 stimulator (Astro-Med, West Warwick, Rhode Island) as descried previously (17,18). Because of the variable responses of BP change to HF stimulation in each dog, we therefore applied HF stimulation to the LSG at 4 incremental levels (level 1 = 1 to 4 V; level 2 = 5 to 7 V; level 3 = 7.5 to 10 V; level 4 = 10 to 15 V).

MEASUREMENT OF THE LSG NEURAL ACTIVITY. Neural activity from the LSG was recorded for 1 minute. A tungsten-coated microelectrode was inserted into the LSG, and a ground lead was connected to the chest wall. The electrical signals generated by the LSG were recorded using a Power Lab data acquisition system (8/35, AD Instruments, Bella Vista, Australia) and amplified by an amplifier (DP-304, Warner Instruments, Hamden, Connecticut) with bandpass filters set at 300 Hz to 1 kHz and an amplification range of 30 to 50 times. Neural

ABBREVIATIONS AND ACRONYMS

AAV = adeno-associated virus
APD = action potential duration
APD90 = 90% repolarization duration
BP = blood pressure
ECG = electrocardiography
ERP = effective refractory period
GFP = green fluorescent protein
HF = high frequency
HRV = heart rate variability
LED = light-emitting diode
LF = low frequency
LSG = left stellate ganglion
NGF = nerve growth factor
Smax = maximum slope of the curve
TH = tyrosine hydroxylase
VA = ventricular arrhythmia
VPB = ventricular premature beat
VT = ventricular tachycardia

FIGURE 1 Study Protocol and GFP/GFP-ArchT Expression Analyses in the LSG

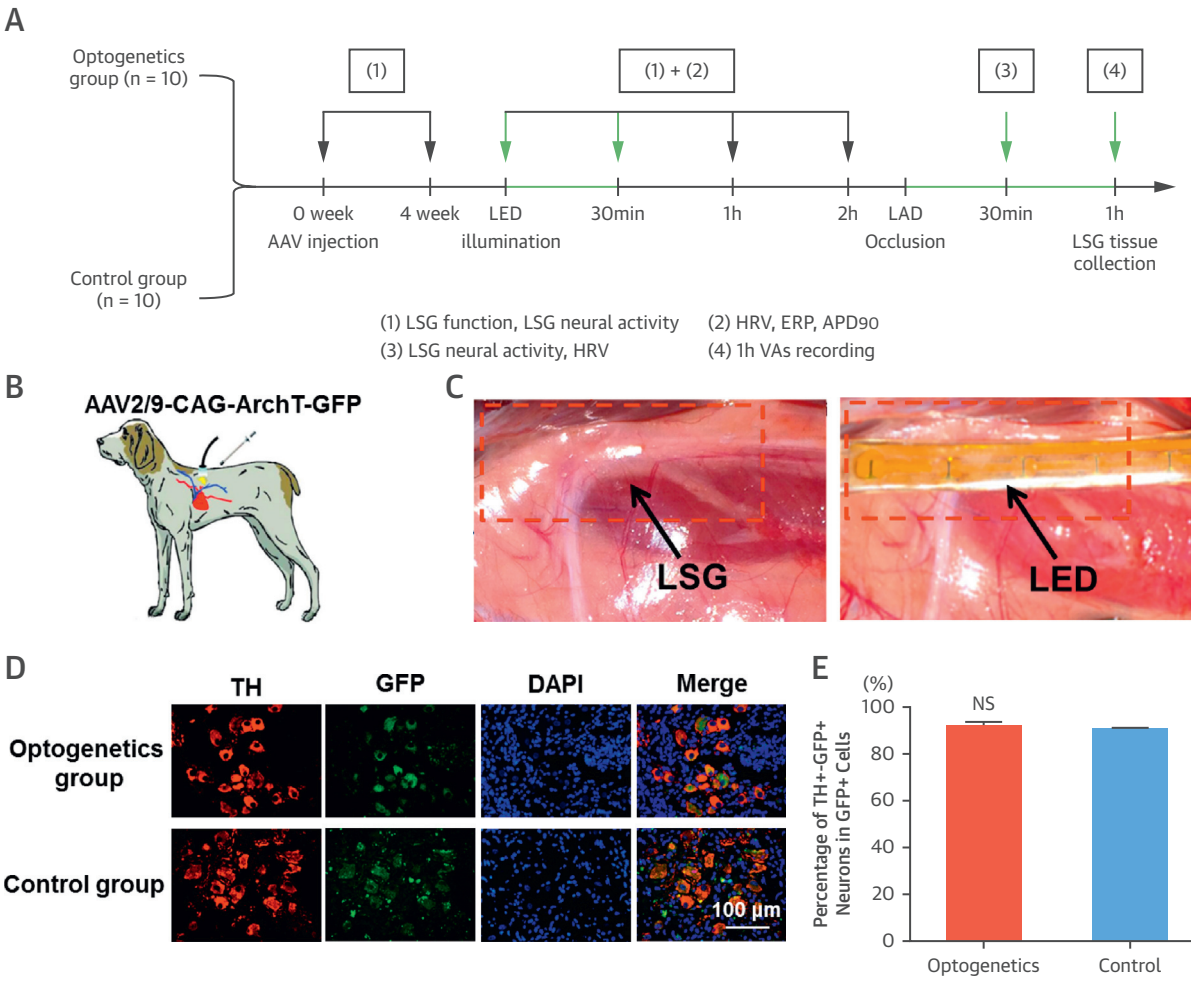

(A) Experimental design flowchart, **(B)** schematic representation of the position of virus microinjection, and **(C)** light-emitting diode (LED) electrode. **(D, E)** Immunofluorescent analyses revealed the successful expression of GFP/GFP-ArchT in the left stellate ganglion (LSG) in both groups. Scale bar = 100 μm. AAV = adeno-associated virus; APD90 = 90% repolarization duration; DAPI = 4′,6-diamidino-2-phenylindole; ERP = effective refractory period; GFP = green fluorescent protein; HRV = heart rate variability; LAD = left anterior descending artery; MAP = monophasic action potential; NS = not significant; TH = tyrosine hydroxylase; VAs = ventricular arrhythmias.

activity, characterized by the recorded amplitude and frequency, was defined as deflections with a signal-to-noise ratio of 3:1 and manually determined as described previously (17-19).

MEASUREMENT OF THE VENTRICULAR EFFECTIVE REFRACTORY PERIOD. Multielectrode catheters were sutured at 3 epicardial sites on the left ventricle. The ventricular effective refractory period (ERP) was determined from the following 3 sites: left ventricular apex, left ventricular base, and the mid left ventricle (the site in the middle of the left ventricular apex and base). The ERP at each site was determined by programmed stimulation consisting of 8 consecutive stimuli (S1-S1, 330 ms cycle length) followed by a premature stimulus (S2). The S1-S2 interval was decreased initially from 250 ms by decrements of 10 ms and then 2 ms until refractoriness was achieved. ERP was defined as the longest S1-S2 interval that failed to capture the ventricles (17,18,20).

MONOPHASIC ACTION POTENTIAL RECORDING. Monophasic action potentials of the left ventricle were recorded from 3 epicardial sites (left ventricular apex, the site in the middle of the left ventricular apex and base, and left ventricular base) using a custom-made Ag-AgCl catheter. A dynamic

steady-state pacing protocol (S1-S1) was performed to determine action potential duration (APD) restitution properties. The pulse train was delivered at an initial cycle length that was slightly shorter than the sinus cycle length, and was maintained for 30 s to ensure a steady state. A 2-min interruption was then taken to minimize the pacing memory effects. Subsequently, another pulse train with the pacing cycle length decreased by 10 ms was delivered until APD alternans appeared. APD alternans was defined as the change in 90% repolarization duration (APD90) ≥10 ms for ≥5 consecutive beats. The monophasic action potential recordings were analyzed by the LEAD 7000 workstation system (Lead 7000, Jinjiang). The APD90 was defined as the 90% repolarization duration, and the diastolic interval was the time interval from the previous APD90 point to the activation time of the next beat. As described in previous studies, the dynamic APD restitution curves were constructed by plotting each APD90 against the preceding diastolic interval using Origin 8.0 (OriginLab, Northampton, Massachusetts). The slope of the shortest diastolic interval was defined as the maximum slope of the curve (Smax) (18,20,21).

MEASUREMENT OF HEART RATE VARIABILITY. Five-minute electrocardiogram segments were recorded to analyze the spectral power for heart rate variability (HRV) using the autoregressive algorithm. The following power spectral variables were determined: the HF, the low frequency (LF), and the LF/HF ratio (18).

MEASUREMENT OF THE MYOCARDIAL ISCHEMIA–INDUCED VENTRICULAR ARRHYTHMIAS. Myocardial ischemia was induced by left anterior descending coronary artery ligation at approximately 2 cm away from its origin. The ECG during the first hour of ischemia was recorded to analyze the incidence and duration of the VAs according to the Lambeth Conventions. VAs were classified as ventricular premature beats (VPBs), nonsustained ventricular tachycardia (VT), and sustained VT and ventricular fibrillation (18,22).

HISTOPATHOLOGIC STAINING. At the end of the experiment, the LSG was resected for histopathologic staining. Tissues were fixed in 4% paraformaldehyde, embedded in paraffin and sectioned into 4-μm slices. Double immunofluorescence staining was used for tyrosine hydroxylase (TH) (Abcam, Cambridge, United Kingdom) with green fluorescent protein (GFP) (Abcam), c-fos (Abcam), and nerve growth factor (NGF) (Abcam). The nuclei were stained with 4,6-diamidino-2-phenylindole.

STATISTICAL ANALYSIS. All continuous variables were presented as the mean ± SEM and tested for a normal distribution using the Shapiro-Wilk normality test. The continuous variables measured at different time points were compared in the 2 groups (Figures 2 to 5) using 2-way repeated-measures analysis of variance followed by Tukey's post hoc test. For histologic analysis and VAs (VPB, nonsustained VT), an unpaired Student's *t*-test was used to compare the means between the 2 groups. For categorical variables, the incidence of sustained VT and ventricular fibrillation between the 2 groups was compared by Fisher exact test. All data were analyzed using GraphPad Prism software version 6.0 (GraphPad Software, La Jolla, California), and $p < 0.05$ was considered statistically significant.

RESULTS

VERIFICATION OF ArchT EXPRESSION IN LSG. LSG slices were costained with anti-TH to label sympathetic neurons and with anti-GFP to label GFP/GFP-expression ArchT. The results showed that GFP was mainly expressed in the TH+ neurons in the LSG in both optogenetics and control groups, verifying the successful GFP/ArchT transfection into LSG sympathetic neurons (Figure 1D). Quantification of the overlap between the TH+ and GFP+ cells revealed that 91.82 ± 1.88% of GFP+ cells were TH+ in the optogenetics group and 90.24 ± 1.22% of GFP+ cells were TH+ in the control group (Figure 1E).

OPTOGENETIC MODULATION SIGNIFICANTLY INHIBITED THE LSG FUNCTION. The LSG function (assessed by the maximal systolic BP change in response to LSG electrical stimulation) (Figure 2A) was significantly attenuated by transient and 30 min of LED illumination in the optogenetics group, and the voltage-BP response curve was significantly flattened by transient or sustained optogenetic modulation (Figures 2D and 2E). For example, the maximal systolic BP change during LSG stimulation at voltage of level 4 (10 to 15 V) decreased from 60.9 ± 2.1% to 37.6 ± 1.8% with transient LED illumination and further decreased to 20.0 ± 0.8% after 30 min of illumination. Two h after illumination was turned off, the LSG function recovered to the baseline level before illumination (62.0 ± 2.5%) (Figure 2G). However, no significant changes in maximal systolic BP change or the voltage-BP response curve were observed in the control group (Figures 2B to 2G).

OPTOGENETIC MODULATION SIGNIFICANTLY INHIBITED THE LSG NEURAL ACTIVITY. During illumination (565 nm), the in vivo neural activity recording showed an evident inhibition of LSG neural

FIGURE 2 Effects of Optogenetic Modulation on LSG Function

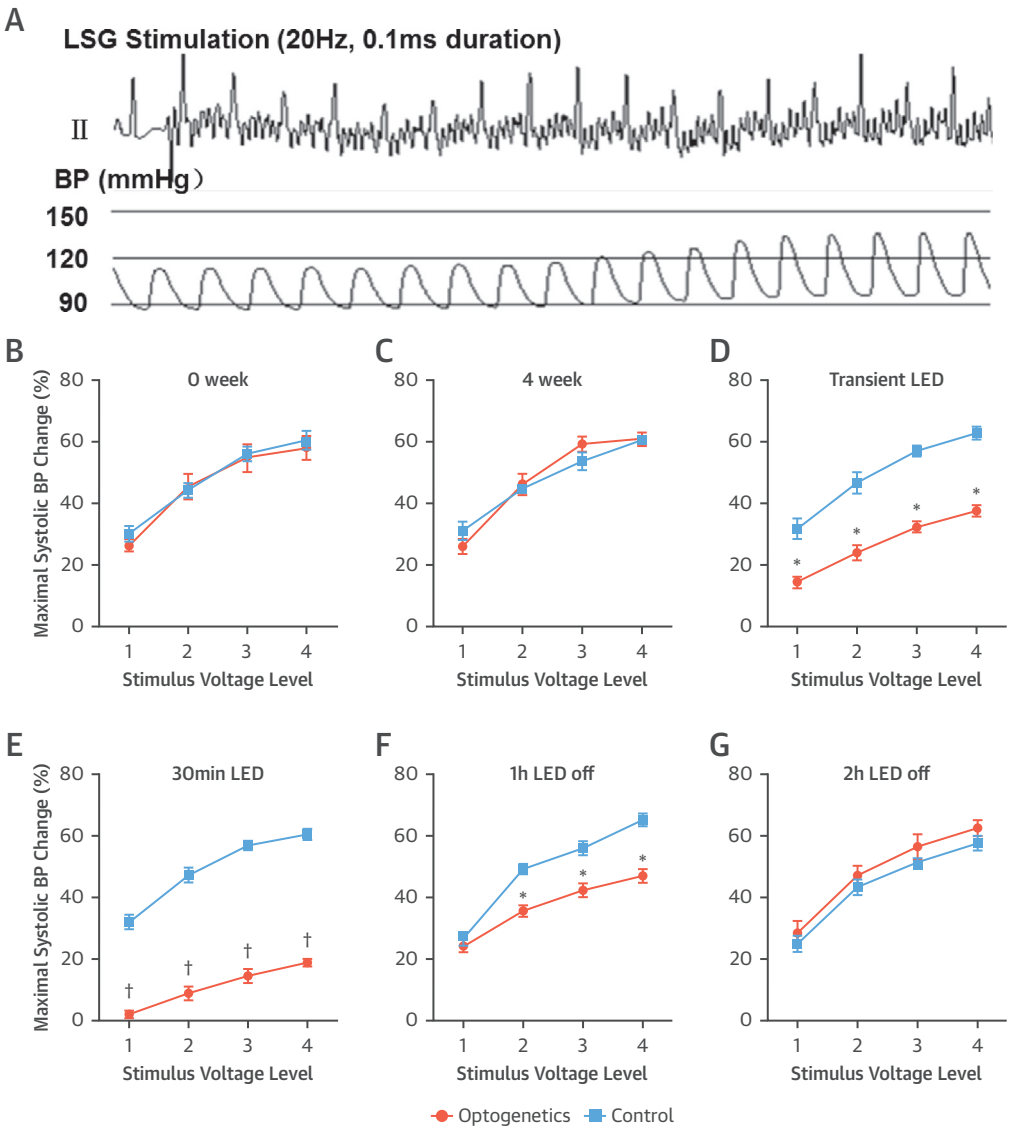

(A) Representative examples of blood pressure (BP) elevation with LSG stimulation. **(B to E)** Transient and 30-min sustained LED illumination significantly decreased LSG function in the optogenetics group. **(F, G)** The decreased LSG function recovered to baseline within 2 h after LED illumination was turned off. *p < 0.05 vs. 4 weeks after viral injection; †p < 0.05 vs. transient LED. Abbreviations as in Figure 1.

activity by transient optogenetic modulation (Figure 3A). Figure 3B showed representative examples of LSG neural activity recordings at different time points in both groups. Transient optogenetic modulation significantly decreased the frequency and amplitude of LSG neural activity (frequency: 47 ± 4 impulses/min vs. 29 ± 4 impulses/min; amplitude: 0.114 ± 0.012 mV vs. 0.063 ± 0.005 mV; $p < 0.05$) in the optogenetics group (Figures 3C and 3D). Thirty minutes of illumination further decreased the LSG neural activity (frequency: 11 ± 3 impulses/min; amplitude: 0.015 ± 0.006 mV). Furthermore, the neural activity of LSG recovered to baseline within 2 h after illumination was turned off (frequency: 45 ± 5 impulses/min; amplitude: 0.114 ± 0.013 mV). However, no significant changes were observed in the control group (Figures 3C and 3D). In addition, the ischemia-induced increase of LSG neural activity was significantly attenuated by optogenetic modulation in the optogenetics group (frequency: 98 ± 6 impulses/min

FIGURE 3 Effects of Optogenetic Modulation on LSG Neural Activity

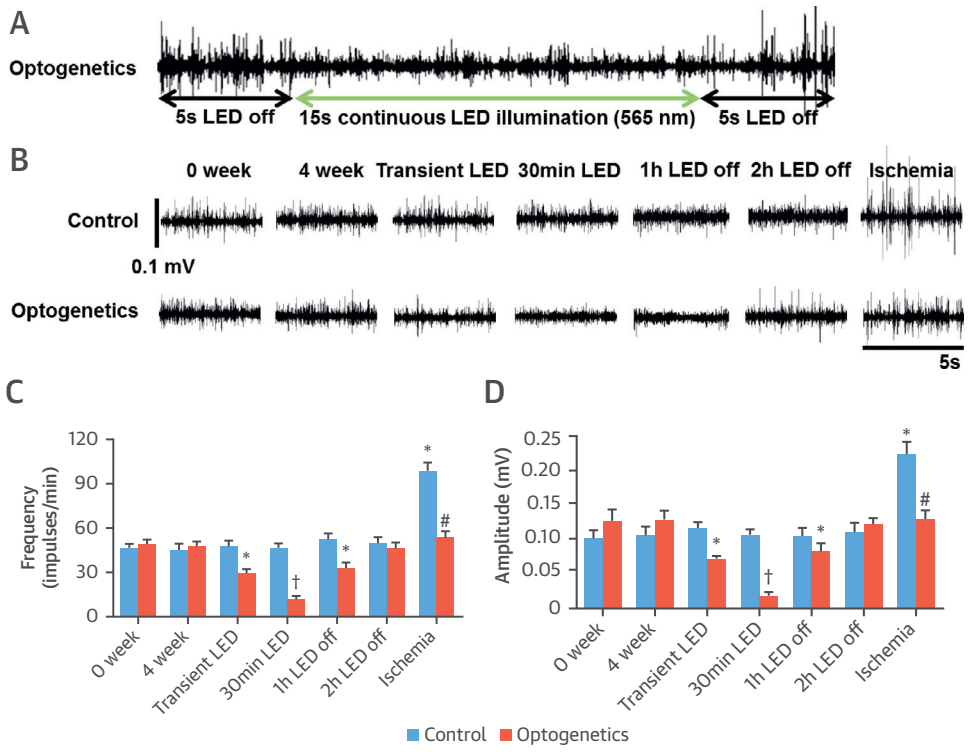

(A, B) Representative examples of optogenetic inhibition of LSG neural activity and **(C, D)** quantitative analysis of LSG neural activity in 2 groups. Transient and sustained LED illumination significantly decreased the frequency and amplitude of LSG neural activity in the optogenetics group. **(C, D)** The decreased LSG neural activity recovered to baseline within 2 h after LED illumination was turned off. In addition, the ischemia-induced increase of LSG neural activity was also attenuated by optogenetic modulation in the optogenetics group. *$p < 0.05$ vs. 4 weeks after virus injection. †$p < 0.05$ vs. transient LED. #$p < 0.05$ vs. control group. Abbreviations as in Figure 1.

vs. 53 ± 5 impulses/min; amplitude: 0.198 ± 0.017 mV vs. 0.114 ± 0.01 mV; $p < 0.05$) (Figures 3C and 3D).

OPTOGENETIC MODULATION SIGNIFICANTLY STABILIZED THE VENTRICULAR ELECTROPHYSIOLOGIC PROPERTIES. Figure 4A shows representative examples of action potential recordings in the optogenetics group. Transient optogenetic modulation significantly prolonged ERP (Figures 4B to 4D) and APD90 (Figures 4E to 4G) and decreased Smax (Figures 4H to 4J) of the left ventricle in the optogenetics group (Figures 4A to 4I). Thirty-minute illumination further enhanced these changes. Moreover, all these electrophysiological changes returned to the baseline level within 2 h after illumination was turned off. Notably, no significant changes in ERP, APD90, or Smax were observed in the control group.

OPTOGENETIC MODULATION SIGNIFICANTLY DECREASED THE SYMPATHETIC INDICES OF HRV. In the optogenetics group, both the LF and the LF/HF ratio were significantly decreased by either transient or 30-min illumination. Moreover, all these changes returned to baseline within 2 h after illumination (Figures 5A and 5C). However, no significant change was found in the LF or the LF/HF ratio in the control group. Similarly, the optogenetic approach significantly attenuated ischemia-induced increase in the LF and the LF/HF ratio and significantly attenuated ischemia-induced decrease in the HF (Figures 5A to 5C).

OPTOGENETIC MODULATION SIGNIFICANTLY DECREASED MYOCARDIAL ISCHEMIA–INDUCED VAs. All dogs developed ECG ST-segment elevation or T-wave changes shortly after left anterior artery occlusion. A synchronous LED illumination was performed in the optogenetics group and sustained for 1 h. Acute myocardial ischemia induced VAs (Figure 6A). As compared with the control group, optogenetic modulation significantly decreased the number of VPBs and nonsustained VT in the optogenetics group

FIGURE 4 Effects of Optogenetic Modulation on Left Ventricular Electrophysiological Properties

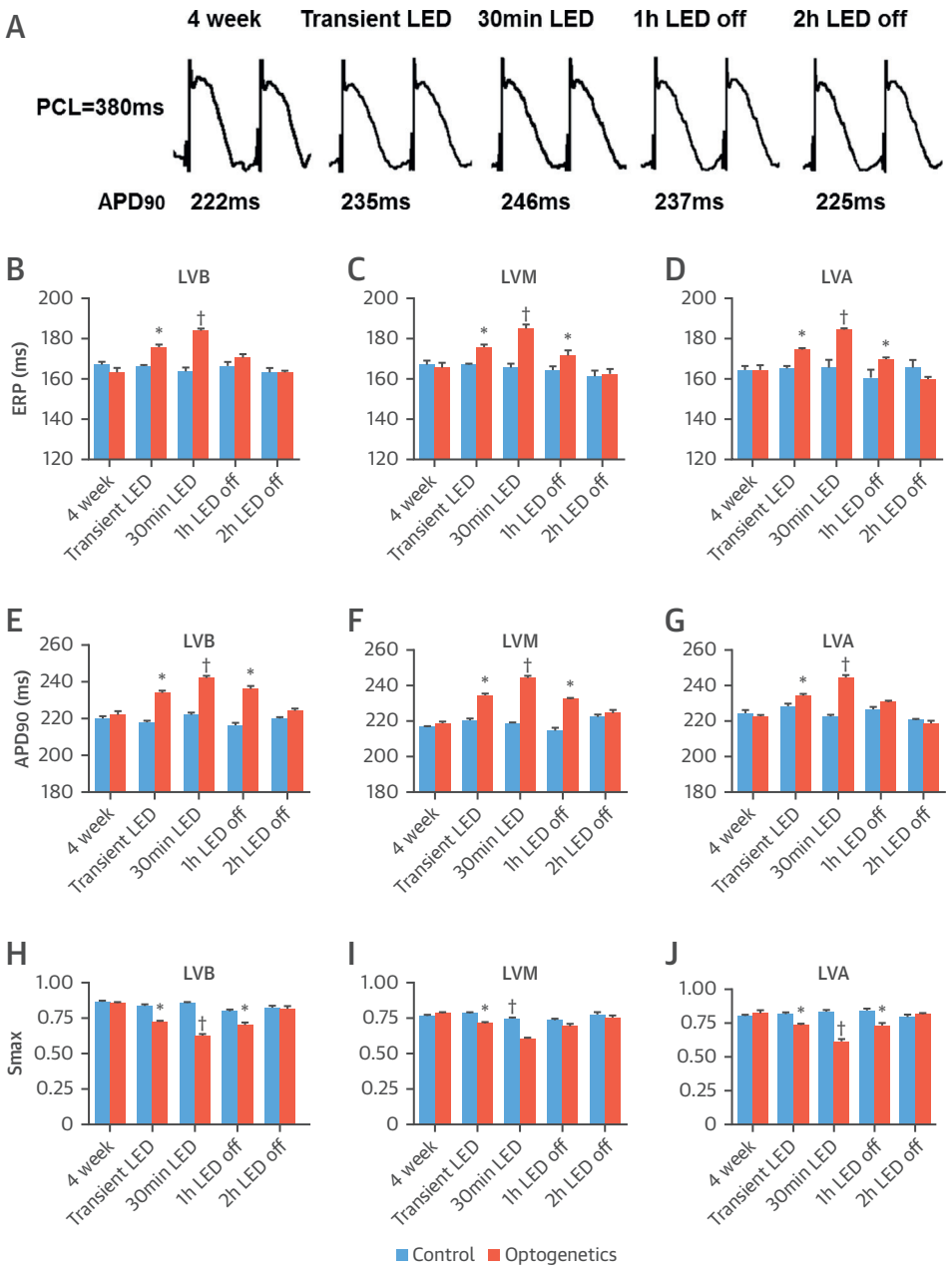

(A) Representative examples of action potential recordings in the optogenetics group. **(B to G)** Optogenetic modulation significantly prolonged left ventricular ERP and APD90, and **(H to J)** decreased the maximal slope of the restitution curve (Smax) in the optogenetics group. All these changes recovered to baseline within 2 h after illumination was turned off. *$p < 0.05$ vs. 4 weeks after virus injection. †$p < 0.05$ vs. transient LED. LVA = left ventricular apex; LVB = left ventricular base; LVM = the median of the left ventricle; PCL = pacing cycle length; other abbreviations as in Figure 1.

(Figures 6B and 6C). The incidence of sustained VT or ventricular fibrillation in the optogenetics group was also lower than that in the control group (2 of 10 [20%] vs. 7 of 10 [70.0%]; $p < 0.05$) (Figure 6D).

OPTOGENETIC MODULATION SIGNIFICANTLY DOWN-REGULATED THE EXPRESSION OF NGF AND C-FOS IN THE LSG. Figures 7A and 7B show representative examples of double immunofluorescence

FIGURE 5 Effects of Optogenetic Modulation on Heart Rate Variability

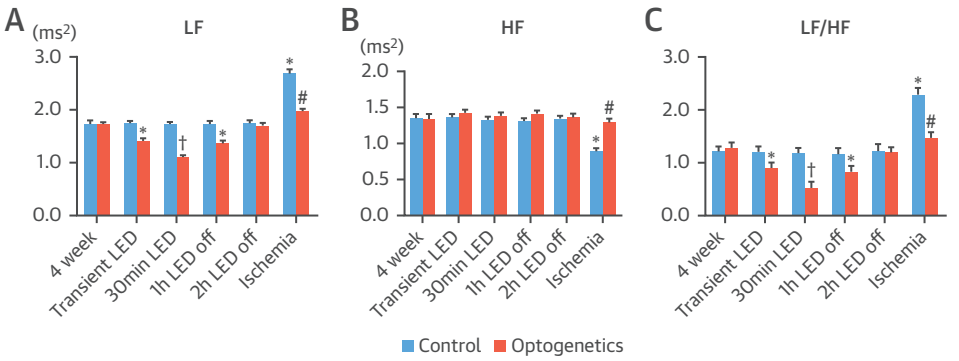

(A, C) Optogenetic modulation significantly decreased the low frequency (LF) and the ratio of the LF and high frequency (HF) in the optogenetics group. All these changes recovered to baseline within 2 h after LED illumination was turned off. **(A to C)** Moreover, optogenetic modulation attenuated the ischemia-induced increase in the LF and the LF/HF ratio, and decrease in the HF. *p < 0.05 vs. 4 weeks after viral injection. †p < 0.05 vs. transient LED. #p < 0.05 vs. control group. LED = light-emitting diode.

staining of NGF/c-fos with TH in both groups. Quantity analysis showed that NGF and c-fos in the LSG were significantly more decreased in the optogenetics group than were those in the control group (NGF: 65.2 ± 4.3% vs. 18.9 ± 2.4%, p < 0.05; c-fos: 73.1 ± 4.5% vs. 22.2 ± 2.6%, p < 0.05) (**Figures 7C and 7D**).

DISCUSSION

MAJOR FINDINGS. In the present study, we demonstrated an effective and reversible optogenetic modulation to inhibit the LSG neural activity and suppress ischemia-induced VAs. We found that transient LED illumination activated the ArchT pump expressed in the LSG neurons, thereby significantly inhibiting the LSG function and neural activity. The sympathetic component of HRV was suppressed. The stability of ventricular electrophysiological properties, measured by the ERP and APD restitution curve, was enhanced as well. Such effects were further enhanced by 30 min of illumination. Moreover, all the aforementioned changes returned to the baseline level within 2 h after illumination was turned off. Importantly, increased LSG neural activity and VAs after myocardial ischemia challenges were significantly decreased by the optogenetic modulation as well. To our best knowledge, this is the first study to apply the optogenetic technology to cardiac autonomic neurons to suppress arrhythmias in vivo.

Currently, cardiac applications of optogenetics were focused on controlling different types of cardiac cells for cardiac pacing, defibrillation or cardioversion, arrhythmia termination, and cell communication research (23-29). Transgenic animals and the AAV-based gene transfer method have been used for expressing of the light-sensitive proteins in vitro and in vivo to facilitate optogenetic control. Wengroski et al. (30) investigated the optogenetic control of norepinephrine release from cardiac sympathetic neurons and its effects on cardiac electrical and mechanical function. They expressed the light-activated optogenetic channel channelrhodopsin-2 in cardiac sympathetic neurons so that the sympathetic fibers could be activated by optogenetic stimulation. The results revealed that exposure to optical activation of the cardiac sympathetic fibers significantly increased norepinephrine release, heart rate, and contractile force; shortened action potentials; and made the heart more susceptible to arrhythmia with greater incidence and severity. This study provided an innovative model and new results that contribute to the mechanism of cardiac sympathetic activation and arrhythmia.

In view of the important role of cardiac sympathetic nervous system on the genesis and maintenance of arrhythmia, left cardiac sympathetic denervation has been applied to treat post-ischemia refractory VAs or electrical storm, long QT syndrome, and catecholaminergic polymorphic VT (6-9). However, there are some side effects associated with this traumatizing and irreversible operation such as unilateral hand dryness, abnormal sweating, and chest pain (31). In the present study, we applied a

FIGURE 6 Effects of Optogenetic Modulation on Myocardial Ischemia–Induced VAs

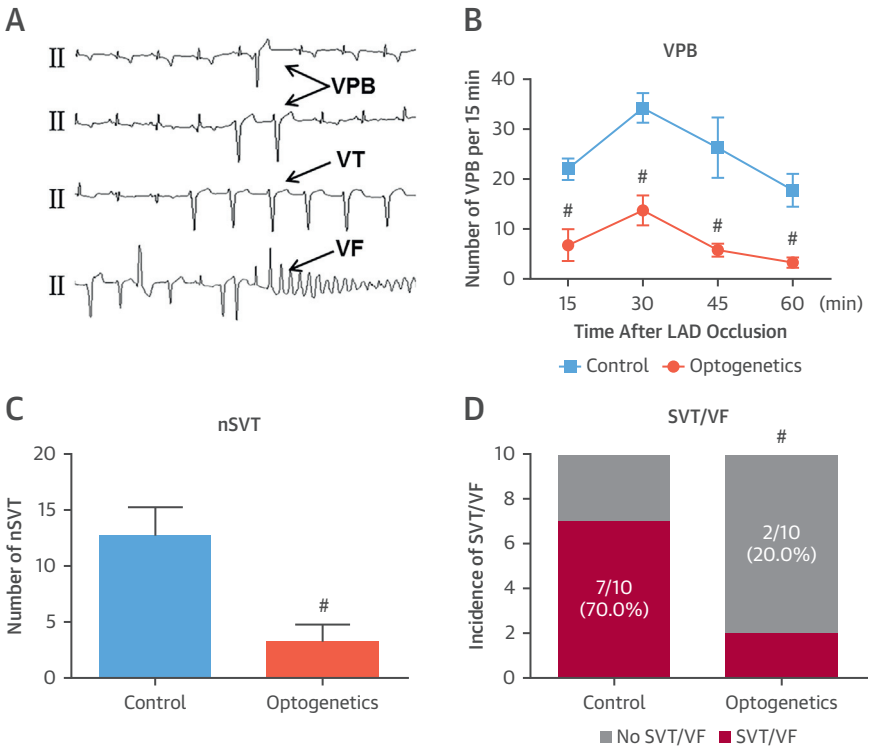

(A) Representative examples of ischemia-induced VAs. **(B)** Quantitative analysis of the incidence of ischemia-induced VAs showed that optogenetic modulation significantly decreased the number of ventricular premature beats (VPBs) and **(C)** nonsustained ventricular tachycardia (nSVT), and **(D)** the incidence of sustained VT (SVT) and ventricular fibrillation (VF) in the optogenetics group. Abbreviations as in Figure 1.

novel and reversible intervention, optogenetics, to modulate the LSG neural activity. The inhibitory light-sensitive protein utilized in our present study is ArchT, a novel light-driven outward proton pump that is sensitive to green light illumination. When genetically expressed in neurons and activated by LED illumination, ArchT discharges H^+ into the extracellular environment, thus causing hyperpolarization and neural silencing (12-14).

Recently, several studies have investigated the inhibitory effect of ArchT on dorsal root ganglion neural activity and neuropathic pain. The results showed that ArchT could be activated in dorsal root ganglion neurons after viral vector administration, thereby inducing a large outflux of H^+, producing hyperpolarization, reducing excitability of the opsin-expressed neurons, and reducing mechanical pain hypersensitivity in a neuropathic pain model. Furthermore, activation of ArchT can be turned on or off by adjusting illumination (32-34).

AAV is one of the most widely used gene therapy vectors with stable and safe gene expression, low immunogenicity, and absence of toxicity (35,36). For instance, AAV serotype 9 was effective at transducing the neurons in the enteric autonomic nervous system (37,38). Therefore, we chose AAV2/9 to transfect LSG and deliver ArchT protein into the LSG neurons. Moreover, we directly injected AAV2/9 vectors into the LSG so that the viral infection and ArchT expression could be limited locally in LSG. The results in the present study demonstrated that ArchT was successfully expressed in the LSG, and that viral infection or gene transfer with AAV2/9 did not alter the LSG function and neural activity.

We investigated the effect of optogenetic inhibition of LSG neurons and assessed this inhibitory effect of LSG on ventricular electrophysiology and VAs in normal and myocardial ischemia canines. Direct neural recordings showed that ArchT

FIGURE 7 Effects of Optogenetic Modulation on c-Fos and NGF Expression in the LSG

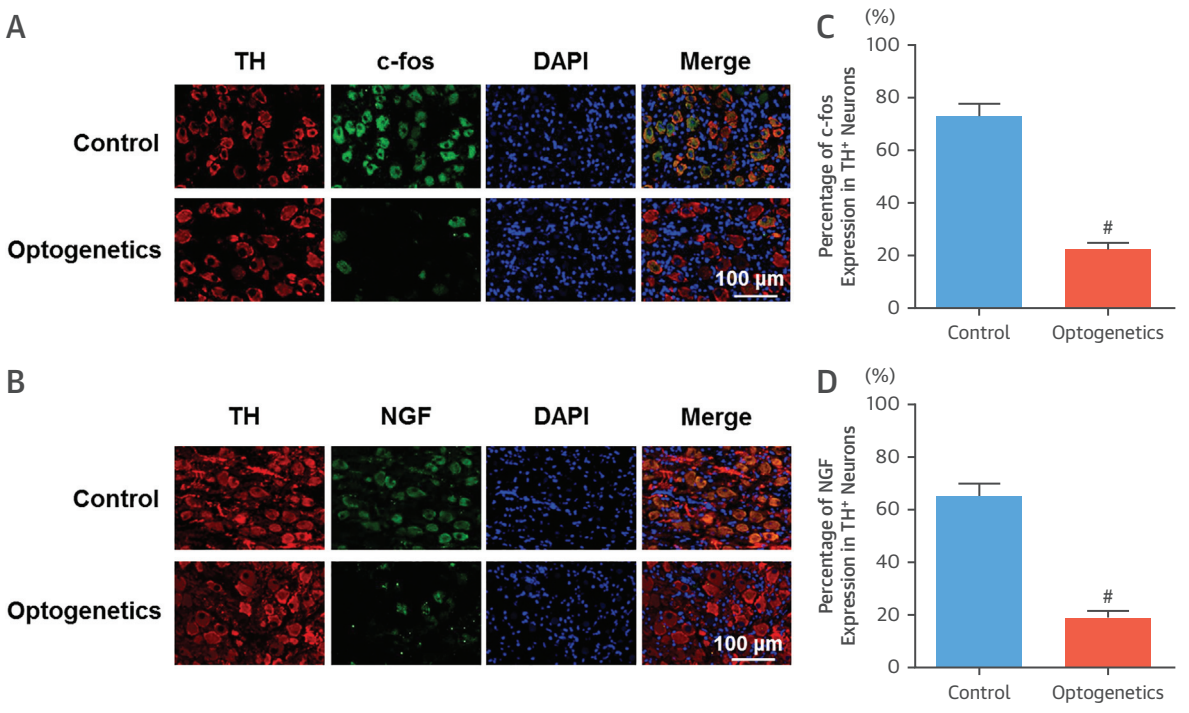

(A, B) Representative immunofluorescent costaining of c-fos/nerve growth factor (NGF) with TH in LSG in both groups. **(C, D)** Quantitative analysis showed that optogenetic modulation significantly down-regulated the expression of c-fos/NGF in TH+ neurons in the LSG in the optogenetics group. #$p < 0.05$ vs. control group. Abbreviations as in Figures 1 and 2.

activation by LED illumination significantly inhibited the neural activity of the LSG in normal and myocardial ischemia canines. The LSG function measured by maximal systolic BP change in response to LSG electrical stimulation was also inhibited by ArchT activation. Furthermore, the expression of NGF and c-fos was significantly decreased by sustained ArchT activation with LED illumination, which may underlie the prolonged inhibitory effect of optogenetic modulation on LSG neural activity. These results all imply that activation of ArchT with illumination might result in an inhibition of LSG neural activity, thereby stabilizing the ventricular electrophysiological properties and suppressing the ischemia-induced VAs.

One concern for long-term LED illumination is heat generation. Researches have revealed that an optical power intensity of 10 mW/mm^2 did not cause detectable temperature changes (16). In view of the great light sensitivity of ArchT, the intensity of light (3 to 5 mW/mm^2) used in this study was small to avoid any thermal damage to LSG and collateral tissues. Importantly, the reversibility of the measured LSG function and neural activity as well as the electrophysiological properties after LED illumination was turned off strongly indicates that thermal injury to the LSG neuron plays a negligible role in the findings we observed.

CLINICAL IMPLICATIONS. Most recently, Montgomery et al. (15) and Park et al. (16) reported the development of implantable wireless optogenetic devices that combined tiny soft neural interfaces with fully implantable stretchable wireless radio power and control systems. These tiny, delicate devices can be implanted with minimally invasive techniques and optogenetically modulate the spinal cord and peripheral nervous system. Optogenetics can potentially become a novel minimally invasive patient-controlled technology for treating cardiovascular diseases related to hyperactivity of the cardiac sympathetic nervous system (**Central Illustration**). For example, the patient may turn on the LED illumination before physical or emotional stress to avoid VAs or defibrillator therapy.

CENTRAL ILLUSTRATION **Optogenetic Modulation Inhibits LSG Neural Activity and Suppresses Ventricular Arrhythmias**

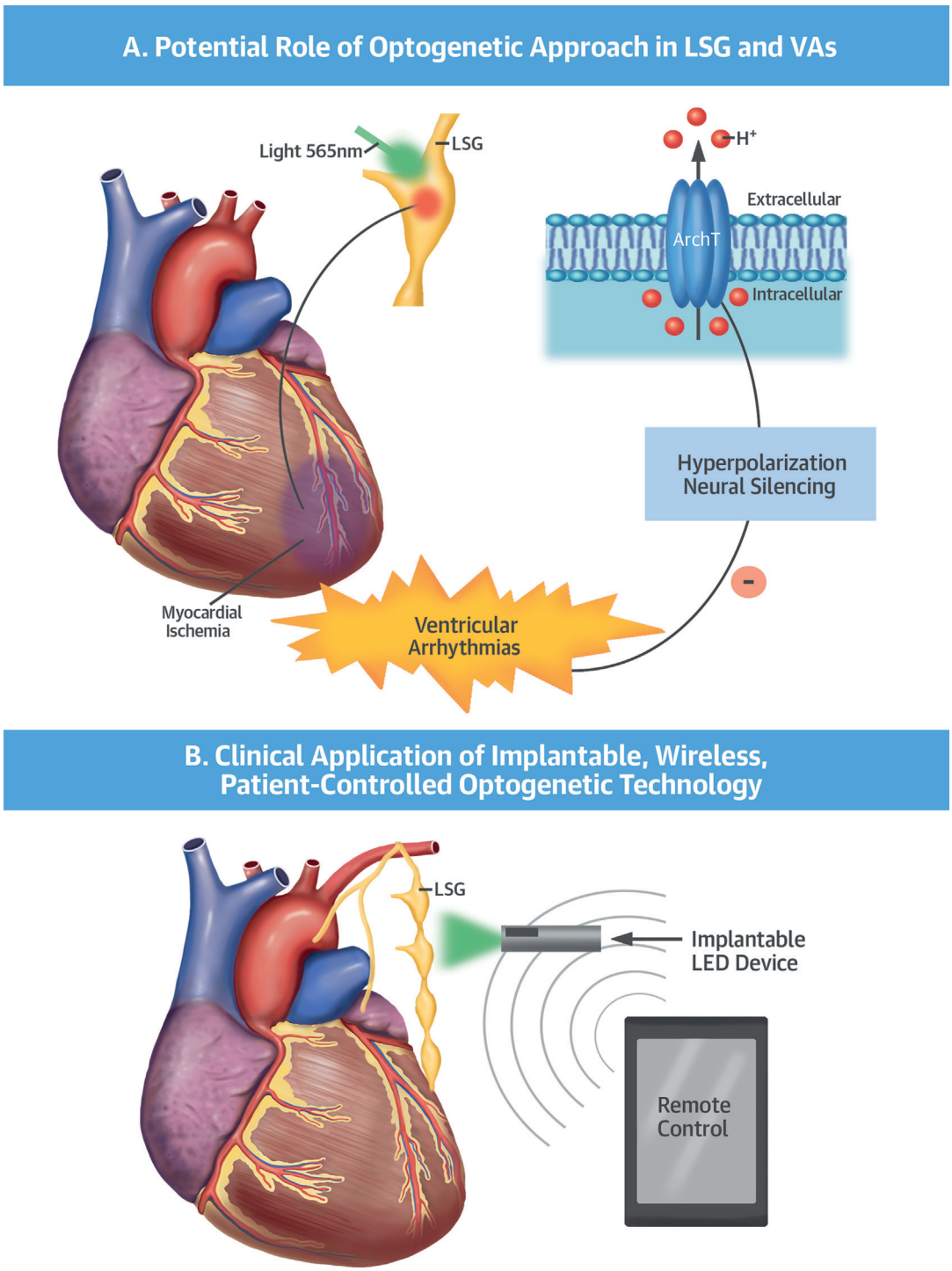

Yu, L. et al. J Am Coll Cardiol. 2017;70(22):2778–90.

(A) We demonstrated for the first time that optogenetics could reversibly inhibit left stellate ganglion (LSG) neural activity and suppress ventricular arrhythmias (VAs) induced by myocardial ischemia. **(B)** Wireless optogenetics may become a novel minimally invasive patient-controlled technology for treating cardiovascular diseases related to hyperactivity of the cardiac sympathetic nervous system. LED = light-emitting diode.

STUDY LIMITATIONS. This study investigated the optogenetic modulation of LSG neural activity. As a proof-of-concept study, we only investigated the efficacy of optogenetic modulation by transfecting LSG with AAV at a fixed titer and dosage. Further dose-effect studies are warranted to investigate the correlation between transfection efficiency and neural modulation. Because of the limitation of LED device and neural recording instruments, we could only perform LED illumination and synchronous neural recording under anesthesia. Furthermore, we only made a short-term study of the optogenetic modulation of LSG neural activity and ischemia-induced VAs in an acute myocardial ischemia canine model. Implantable wireless optogenetic devices and neural recording instruments are warranted to investigate the precise control of optogenetics on the cardiac autonomic nervous system and VAs in ambulatory chronic myocardial ischemia models.

CONCLUSIONS

Optogenetic technology could reversibly and controllably modulate LSG neural activity and thus suppress VAs induced by myocardial ischemia. Optogenetics may become a novel minimally invasive patient-activated technology for treating cardiovascular diseases related to hyperactivity of the cardiac sympathetic nervous system.

ADDRESS FOR CORRESPONDENCE: Dr. Hong Jiang, Department of Cardiology, Renmin Hospital of Wuhan University, No. 238 Jiefang Road, Wuchang District, Wuhan City, Hubei Province 430060, P. R. China. E-mail: hong-jiang@whu.edu.cn.

PERSPECTIVES

COMPETENCY IN MEDICAL KNOWLEDGE: In a canine model of myocardial ischemia, optogenetic modulation reversibly silenced stellate ganglion sympathetic nerve activity and significantly suppressed VAs.

TRANSLATIONAL OUTLOOK: Further studies are warranted to explore the safety and efficacy of wireless optogenetic modulation of cardiac autonomic innervation and its potential therapeutic utility in man.

REFERENCES

1. John RM, Tedrow UB, Koplan BA, et al. Ventricular arrhythmias and sudden cardiac death. Lancet 2012;380:1520–9.

2. Priori SG, Blomstrom-Lundqvist C, Mazzanti A, et al. 2015 ESC Guidelines for the management of patients with ventricular arrhythmias and the prevention of sudden cardiac death: the Task Force for the Management of Patients with Ventricular Arrhythmias and the Prevention of Sudden Cardiac Death of the European Society of Cardiology (ESC). Endorsed by: Association for European Paediatric and Congenital Cardiology (AEPC). Eur Heart J 2015;36:2793–867.

3. Schwartz PJ, Vanoli E. Cardiac arrhythmias elicited by interaction between acute myocardial ischemia and sympathetic hyperactivity: a new experimental model for the study of antiarrhythmic drugs. J Cardiovasc Pharmacol 1981;3:1251–9.

4. Puddu PE, Jouve R, Langlet F, Guillen JC, Lanti M, Reale A. Prevention of postischemic ventricular fibrillation late after right or left stellate ganglionectomy in dogs. Circulation 1988;77:935–46.

5. Garcia-Calvo R, Chorro FJ, Sendra M, et al. The effects of selective stellate ganglion manipulation on ventricular refractoriness and excitability. Pacing Clin Electrophysiol 1992;15:1492–503.

6. Schwartz PJ, Stone HL. Left stellectomy in the prevention of ventricular fibrillation caused by acute myocardial ischemia in conscious dogs with anterior myocardial infarction. Circulation 1980;62:1256–65.

7. Vaseghi M, Gima J, Kanaan C, et al. Cardiac sympathetic denervation in patients with refractory ventricular arrhythmias or electrical storm: intermediate and long-term follow-up. Heart Rhythm 2014;11:360–6.

8. Collura CA, Johnson JN, Moir C, Ackerman MJ. Left cardiac sympathetic denervation for the treatment of long QT syndrome and catecholaminergic polymorphic ventricular tachycardia using video-assisted thoracic surgery. Heart Rhythm 2009;6:752–9.

9. Wilde AA, Bhuiyan ZA, Crotti L, et al. Left cardiac sympathetic denervation for catecholaminergic polymorphic ventricular tachycardia. N Engl J Med 2008;358:2024–9.

10. Deisseroth K. Optogenetics. Nat Methods 2011;8:26–9.

11. Yizhar O, Fenno LE, Davidson TJ, Mogri M, Deisseroth K. Optogenetics in neural systems. Neuron 2011;71:9–34.

12. Tsunematsu T, Tabuchi S, Tanaka KF, Boyden ES, Tominaga M, Yamanaka A. Long-lasting silencing of orexin/hypocretin neurons using archaerhodopsin induces slow-wave sleep in mice. Behav Brain Res 2013;255:64–74.

13. Chow BY, Han X, Dobry AS, et al. High-performance genetically targetable optical neural silencing by light-driven proton pumps. Nature 2010;463:98–102.

14. Han X, Chow BY, Zhou H, et al. A high-light sensitivity optical neural silencer: development and application to optogenetic control of non-human primate cortex. Front Syst Neurosci 2011;5:18.

15. Montgomery KL, Yeh AJ, Ho JS, et al. Wirelessly powered, fully internal optogenetics for brain, spinal and peripheral circuits in mice. Nat Methods 2015;12:969–74.

16. Park SI, Brenner DS, Shin G, et al. Soft, stretchable, fully implantable miniaturized optoelectronic systems for wireless optogenetics. Nat Biotechnol 2015;33:1280–6.

17. Wang S, Zhou X, Huang B, et al. Spinal cord stimulation protects against ventricular arrhythmias by suppressing left stellate ganglion neural activity in an acute myocardial infarction canine model. Heart Rhythm 2015;12:1628–35.

18. Wang S, Zhou X, Huang B, et al. Noninvasive low-frequency electromagnetic stimulation of the left stellate ganglion reduces myocardial infarction-induced ventricular arrhythmia. Sci Rep 2016;6:30783.

19. Zhou X, Zhou L, Wang S, et al. The use of noninvasive vagal nerve stimulation to inhibit sympathetically induced sinus node acceleration: a potential therapeutic approach for inappropriate sinus tachycardia. J Cardiovasc Electrophysiol 2016;27:217–23.

20. Huang B, Yu L, He B, et al. Sympathetic denervation of heart and kidney induces similar effects on ventricular electrophysiological properties. EuroIntervention 2015;11:598–604.

21. He B, Lu Z, He W, et al. Effects of ganglionated plexi ablation on ventricular electrophysiological properties in normal hearts and after acute myocardial ischemia. Int J Cardiol 2013;168:86–93.

22. Walker MJ, Curtis MJ, Hearse DJ, et al. The Lambeth Conventions: guidelines for the study of arrhythmias in ischaemia infarction, and reperfusion. Cardiovasc Res 1988;22:447–55.

23. Arrenberg AB, Stainier DY, Baier H, Huisken J. Optogenetic control of cardiac function. Science 2010;330:971–4.

24. Nussinovitch U, Gepstein L. Optogenetics for in vivo cardiac pacing and resynchronization therapies. Nat Biotechnol 2015;33:750–4.

25. Bruegmann T, Boyle PM, Vogt CC, et al. Optogenetic defibrillation terminates ventricular arrhythmia in mouse hearts and human simulations. J Clin Invest 2016;126:3894–904.

26. Crocini C, Ferrantini C, Coppini R, et al. Optogenetics design of mechanistically based stimulation patterns for cardiac defibrillation. Sci Rep 2016;6:35628.

27. Herron TJ, Lee P, Jalife J. Optical imaging of voltage and calcium in cardiac cells & tissues. Circ Res 2012;110:609–23.

28. Nyns EC, Kip A, Bart CI, et al. Optogenetic termination of ventricular arrhythmias in the whole heart: towards biological cardiac rhythm management. Eur Heart J 2017;38:2132–6.

29. Wang Y, Lin WK, Crawford W, et al. Optogenetic control of heart rhythm by selective stimulation of cardiomyocytes derived from Pnmt+ cells in murine heart. Sci Rep 2017;7:40687.

30. Wengrowski AM, Wang X, Tapa S, Posnack NG, Mendelowitz D, Kay MW. Optogenetic release of norepinephrine from cardiac sympathetic neurons alters mechanical and electrical function. Cardiovasc Res 2015;105:143–50.

31. Antiel RM, Bos JM, Joyce DD, et al. Quality of life after videoscopic left cardiac sympathetic denervation in patients with potentially life-threatening cardiac channelopathies/cardiomyopathies. Heart Rhythm 2016;13:62–9.

32. Li B, Yang XY, Qian FP, Tang M, Ma C, Chiang LY. A novel analgesic approach to optogenetically and specifically inhibit pain transmission using TRPV1 promoter. Brain Res 2015;1609:12–20.

33. Boada MD, Martin TJ, Peters CM, et al. Fast-conducting mechanoreceptors contribute to withdrawal behavior in normal and nerve injured rats. Pain 2014;155:2646–55.

34. Daou I, Beaudry H, Ase AR, et al. Optogenetic silencing of Nav1.8-positive afferents alleviates inflammatory and neuropathic pain. eNeuro 2016;3.

35. Mason MR, Ehlert EM, Eggers R, et al. Comparison of AAV serotypes for gene delivery to dorsal root ganglion neurons. Mol Ther 2010;18:715–24.

36. Towne C, Pertin M, Beggah AT, Aebischer P, Decosterd I. Recombinant adeno-associated virus serotype 6 (rAAV2/6)-mediated gene transfer to nociceptive neurons through different routes of delivery. Mol Pain 2009;5:52.

37. Benskey MJ, Kuhn NC, Galligan JJ, et al. Targeted gene delivery to the enteric nervous system using AAV: a comparison across serotypes and capsid mutants. Mol Ther 2015;23:488–500.

38. Dayton RD, Wang DB, Klein RL. The advent of AAV9 expands applications for brain and spinal cord gene delivery. Expert Opin Biol Ther 2012;12:757–66.

KEY WORDS left stellate ganglion neural silencing, optogenetics, ventricular arrhythmia